Heliyon 10 (2024) e39066

Contents lists available at ScienceDirect

Heliyon

journal homepage: www.cell.com/heliyon

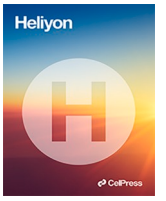

Research article

Theoretical and experimental studies on the electrochemical behavior of steel in HCl solution in the presence of two bio-inhibitor mixtures

Amirhossein Hafazeh [a], Haneih Mobtaker [a], Mahboobeh Azadi [a,*], Maryam Rassouli [b]

[a] Faculty of Materials and Metallurgical Engineering, Semnan University, Semnan, Iran
[b] Pathobiology Department, Shamirzad School of Veterinary Medicine, Semnan University, Semnan, P.O. Box: 35131-19111, Iran

ARTICLE INFO

Keywords:
Bio-inhibitor
Molecular dynamics simulation
Corrosion rate
Monte Carlo calculation
Quinoa seed
Oestrus ovis larvae extract

ABSTRACT

In this new study, the inhibitory effectiveness of two bio-inhibitor mixtures has been studied on the corrosion characteristics of carbon steel in an HCl environment. The inhibitors were derived from a plant seed (*quinoa* seed-QS) and an insect extract (*Oestrus ovis* larvae-OOL). The total inhibitor concentration was a variable factor even the ratio of bio-inhibitor concentration was a fixed parameter. The electrochemical behavior of steel substrate was investigated through the Tafel polarization and electrochemical impedance spectroscopy measurements. Fourier transform infrared spectroscopy and field emission scanning electron microscopy were performed to identify bonds and analyze the morphology of the corroded surface of the steel. Additionally, molecular dynamics (MD) simulation and quantum calculations were applied to investigate the inhibitory influence of utilized bio-inhibitors. The experimental results indicated that the corrosion resistance decreased to 85 % when the optimum total concentration of the bio-inhibitor was 1 g L^{-1}. The Langmuir model was used to illustrate the adsorption mechanism on the steel surface when physical adsorption occurred. Quantum chemical calculations revealed that the QS-inhibitor adsorbed more effectively onto the metal surface than the OOLE-inhibitor, due in part to a lower energy gap and higher HOMO energy. MD simulation and Monte Carlo calculations further confirmed that the QS-inhibitor was adsorbed on the Fe (110) surface with higher adsorption energy than the OOLE-inhibitor.

1. Introduction

Corrosion is a significant problem in many industries, causing product wastage, equipment damage, pollution, and, in severe cases, explosions and harm to human health, the environment, and the economy [1–3]. In the past, numerous studies have been conducted to understand the root causes and various types of corrosion, along with ways to prevent it. While many effective techniques for corrosion prevention and inhibitory chemicals are used nowadays, they often come with side effects on the environment and employees' health in the long run. Despite the challenges, researchers are continuously working towards developing sustainable and safe solutions for corrosion prevention [3–5].

Natural inhibitors are gaining interest among researchers as a safer and more environmentally friendly alternative to traditional

* Corresponding author.
E-mail address: m.azadi@semnan.ac.ir (M. Azadi).

https://doi.org/10.1016/j.heliyon.2024.e39066
Received 31 May 2024; Received in revised form 14 September 2024; Accepted 7 October 2024
Available online 9 October 2024

chemicals. However, it can be challenging to predict the effectiveness of these inhibitors in a particular environment without conducting experiments. Due to their potential toxicity and environmental impact, the use of corrosion inhibitors is tightly regulated [6]. Therefore, it is crucial to analyze the requirements of any media, such as water, fuel, acids, or the atmosphere before using inhibitors, even if they have been used for many years [1,7].

Before the 1960s, the most important factor when selecting corrosion inhibitors was their efficiency. In the following decades, the economy became a key consideration. Nowadays, the environment is also a crucial factor. However, there is still no widely accepted definition of what makes a corrosion inhibitor environmentally friendly. Nevertheless, they should be assessed based on their impact on health, safety, and the environment. Green inhibitors should have low toxicity, quick biodegradation, minimal accumulation, and should not contain harmful elements or compounds [8,9]. Many studies have focused on replacing toxic inhibitors with non-toxic or less toxic alternatives. For example, *Ginkgo* leaf extract [10], *Medicago sativa* [11], *salvia officinalis* [12], Propolis [13], *Sargassum wightii* extract [14], *Aloe vera* extracts [15], and vanillin [16] are all recommended as effective inhibitors to protect steel from corrosion caused by acids.

Inhibitors are usually not used individually, but rather in combination with other compounds to create more effective mixtures. These mixtures are commonly used in cooling systems, acid-washing, and as anodic and cathodic inhibitors. Thus, in this new study, the theoretical and experimental adsorption mechanisms of two bio-inhibitor mixtures on the corrosion behavior of carbon steel were investigated. Finally, the effective concentration of the inhibitor was introduced. These bio-inhibitors were obtained from a plant (*quinoa* seed-QS) as a low-cost, available, and abundant material without any extract process and an insect (*Oestrus ovis* larvae-OOL) extract as an insect-waste and low-cost material. The performance of the inhibitor mixture has been studied in terms of molecular dynamics (MD) simulation, Monte Carlo calculation, and density functional theory (DFT), as well as, potentiodynamic polarization diagrams and electrochemical impedance spectroscopy measurements. Notably, previous articles have individually reported on both inhibitors solely as experimental data [1,2]. However, this paper explores a new scenario by examining the combined effect of these inhibitors at varying concentrations and a constant ratio through experimental data, MD simulations, and other calculations. Both adsorption competition and adsorption persistence of inhibitors have been investigated by MD simulation.

2. Materials and methods

2.1. Initial materials

St 37 carbon steel with chemical composition of 0.8 % Mn, 0.5 % C, 0.3 % Si, and 98.4 % Fe (by weight percent) was used as steel substrate. The chemical composition was measured through spark emission spectroscopy (SES- Hitach Higtech). This steel was applied in various construction components. The quinoa seed and extract of *Oestrus ovis* larvae was chosen as a bio-inhibitor. The basis of this choice was found in our previous studies [1,2]. Both of them included cyclic carbon structure with phenolic groups. The produced *Oestrus ovis* larvae extract powder created using a technique known as Soxhlet extraction. Ethanol was used as a solvent during the process. To prepare the mixture of inhibitor, quinoa seeds, and *Oestrus ovis* larvae extract powder were crushed through a ball-milling (PLM2C-model) device for 30 min. A ceramic cup containing ceramic balls was employed for the process. The diameter of the balls ranged from 10 to 20 mm. The mixing occurred at a temperature of approximately 298 K. The mass ratio of the balls to the powder was set at 10:1, and the milling speed was maintained at around 100 rpm.

In this study, a bio-inhibitor mixture was utilized, and its preparation steps are shown in Fig. 1. The schematic provides a clear overview of the process. The corrosive media was a 1 M HCl solution. Notably, the HCl solution is commonly used in the acid-washing process of important industrial alloys, such as carbon steels. Table 1 provides details on various samples used in the study, including their specific total concentrations of bio-inhibitors. The *Oestrus ovis* larvae extract and quinoa seed were named as OOLE and QS, respectively. Additionally, the ratio of inhibitors was 1:1 in the three chosen concentrations. Since natural inhibitors such as plant extracts exhibit unidentified and several active constituents the applied concentration was usually higher than synthetic inhibitors. For example, the concentration of inhibitor is reported from 0.015 [17] up to 25 g L^{-1} [18].

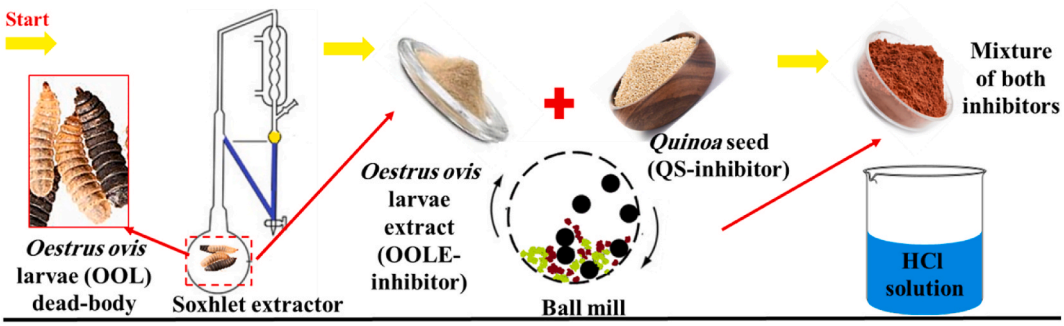

Fig. 1. Schematic of the preparation steps of utilized bio-inhibitor mixture.

Table 1
Detail of various utilized samples.

Sample name	Concentration of OOLE in solution (g L^{-1})	Concentration of QS in solution (g L^{-1})	Total concentration of bio-inhibitor (g L^{-1})
Blank	0	0	0
0.25-OOLE+0.25-QS	0.25	0.25	0.50
0.5-OOLE+0.5-QS	0.50	0.50	1.00
1-OOLE+1-QS	1.00	1.00	2.00

2.2. Experimental part

All samples were ground up to P1000 with SiC sandpaper, washed with acetone, and dried in free air before experiments. The experimental techniques of potentiodynamic polarization (PDP) and electrochemical impedance spectroscopy (EIS) were carried out using an advanced potentiostat device called Organoflex model. The St 37 carbon steel sheet was the working electrode. The working electrode had an exposed area of 1 cm^2, while the reference electrode was a saturated calomel electrode (SCE), and the counter electrode was a platinum thin sheet. Before electrochemical measurements, the open circuit potential (OCP) was scanned for 15 min. And then, EIS measurements were done with a frequency from 100 kHz to 0.01 Hz. The applied potential amplitude was ±10 mV around the measured OCP value. At last, the impedance data was fitted by ZView software. During the PDP tests, the scanning potential was varied from ±250 mV of the measured OCP value, with a scan rate of 1 mV s^{-1}. The experiments were conducted at a constant temperature of 298 K, ensuring consistent and reliable results. For studying the mechanism of adsorption for utilized bio-inhibitors, equation (1) was used.

$$C / \theta = 1/K_{ads} + C \tag{1}$$

Where K_{ads} is a constant corresponding to the adsorption equilibrium, θ is inhibition efficacy, and C is the total concentration of the inhibitor. Significantly, within the PDP test, the parameter θ represents the percentage decrease in the corrosion current density of the steel substrate when the bio-inhibitor is present as opposed to when it is absent. On the other hand, in EIS measurements, θ signifies the percentage increase in the polarization resistance of the steel substrate with the bio-inhibitor present compared to its absence. Further information can be explored in additional literature sources [1–3]. It is important to highlight that the percentage of inhibition efficiency can be determined by multiplying θ by 100.

Moreover, the standard adsorption-free energy (ΔG°_{ads}) can be calculated through equation (2)

$$\Delta G^{\circ}_{ads} = -\mathrm{RTln}\,(1000\,K_{ads}) \tag{2}$$

Where R and T represent the gas constant and the environment temperature, respectively. A similar formula was reported in other research studies [19–21].

The Fourier Transform Infra-Red spectroscopy (FTIR- Shimadzu 8400S) method was performed to detect present bonds in the chemical composition of OOLE and QS molecules. The range of wavenumber was 4000-400 cm^{-1}.

The corroded surface of samples was examined using a field emission scanning electron microscopy (FE-SEM-TeScan Mira 3 model) at a voltage of 15 kV.

2.3. Computational details

2.3.1. Quantum chemical calculations

Quantum chemical calculations based on density functional theory (DFT) is a method to predict the chemical reactivity of inhibitor molecules. Quantum mechanics was performed with Materials Studio software version 2017 and using the DMOL3 module. Optimization of the inhibitor molecule with the DMOL3 module and with the generalized gradient approximation (GGA) with the Perdew-Burke-Ernzerhof (PBE) function using the polarization set a double number (DNP) and Basis file: 3.5 were obtained. The energy of the highest occupied molecular orbital (E_HOMO), the lowest unoccupied molecular orbital (E_LUMO), Fukui indices, and electrostatic potential (ESP) is information that is obtained from quantum calculations. Electron affinity (A), ionization potential (I), hardness (η), softness (χ), energy gap (ΔE), and fraction of transferred electrons (ΔN), were calculated from equations (3)–(8)

$$I = -E_{HOMO} \tag{3}$$

$$A = -E_{LUMO} \tag{4}$$

$$\chi = \frac{I + A}{2} \tag{5}$$

$$\eta = \frac{I - A}{2} \tag{6}$$

$$\Delta N = \frac{\chi_{Fe} - \chi_{inh}}{2(\eta_{Fe} + \eta_{inh})} \tag{7}$$

$$\Delta E = E_{LUMO} - E_{HOMO} \tag{8}$$

Moreover, $\chi_{Fe} = 7\,\frac{ev}{mol}$ and $\eta_{Fe} = 0\,\frac{ev}{mol}$ were considered [1]. To determine the reactivity sites of QS-inhibitor and OOLE-inhibitor molecules, Fukui functions were calculated using the following equations.

$$f_k^+ = P(N+1) - P(N) \tag{9}$$

$$f_k^- = P(N) - P(N-1) \tag{10}$$

$$f_k^0 = [P(N+1) - P(N-1)]/2 \tag{11}$$

where P(N), P(N+1), and P(N-1) represented the charge values in neutral, cation, and anion forms, QS-inhibitor, and OOLE-inhibitor molecules, respectively [22,23].

2.3.2. Molecular dynamics (MD) simulations

The reaction of QS-inhibitor and OOLE-inhibitor molecules with steel surface was theoretically analyzed by MD simulation. Adsorption of inhibitor molecules on Fe (110) surface with dimensions of 29.79 × 29.79 × 35.13 $A^{\circ 3}$ consisting of 6 atomic layers and a 12 × 12 supercell with a vacuum of 25 A° in the C axis and HCl media was done. Similar parameters were also reported in other research [24]. Inhibitor molecules were drawn and optimized with Forcite, and then the adsorption energy was calculated with the Adsorption Locator module. The temperature of the simulation system was controlled by Brandsen thermostat of the NVT group at a temperature of 298 K with a time step of 1 fs and a simulation time of 300 ps under the COMPASS force field [1]. The radial distribution function (RDF) was analyzed with 300 ps frames of trajectory data. A similar function was also used in other paper [25].

3. Results and discussion

3.1. FTIR

Fig. 2 displays FTIR patterns for both bio-inhibitors. The pattern of QS-inhibitor contained O-H, C-H, C=O, -COO, C-H, C-O, and C=O bonds which were located at wavenumbers 3402, 2927, 1641, 1415, 1154, 1026 and 578 cm^{-1}, respectively. OOLE-inhibitor was also included O-H (N-H), C-H, C=O (C-N), C-H, C-O, C-N, C=C and C=O that show peaks at wavenumbers of 3575, 2930, 1651, 1110, 1044, 922, 673, and 563 cm^{-1}, respectively. More details of such patterns were found in previous studies [1,2]. Since iron atoms exhibited free d-orbital, molecules with lone pairs of electrons, molecules with double bonds, and cyclic carbon structures were agents that could be adsorbed on the metal surfaces [26,27].

3.2. PDP results

Fig. 3(a) indicates plots of OCP versus the immersion time for various samples. The OCP with a value of −510 mV for the blank sample was the most negative potential, displaying the highest thermodynamic tendency to corrosion attacks. Adding the bio-inhibitors to the solution, increased OCP values, and the highest value related to the sample 1-OOLE+1-QS. Such a value showed that in the presence of the bio-inhibitor in the corrosive solution, the steel surface exhibited a lower tendency to corrosion reactions. It is worth noting that similar observations have been reported in other research studies [28,29]. Overall, the range of OCP values for all samples was found to be between −480 and −510 mV.

Fig. 3(b) shows plots of log i_{corr} versus the potential as the PDP results. The corrosion rate of steel substrate decreased in the

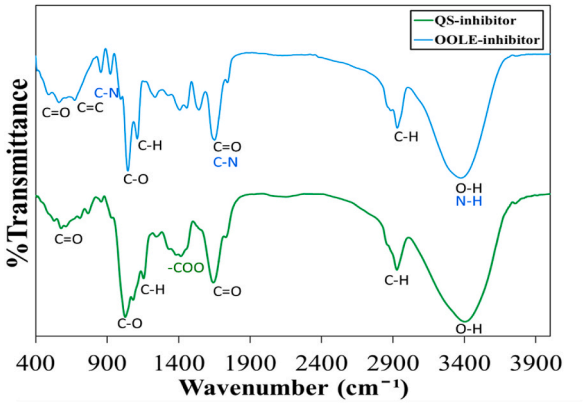

Fig. 2. FTIR patterns for QS-inhibitor and OOLE-inhibitor.

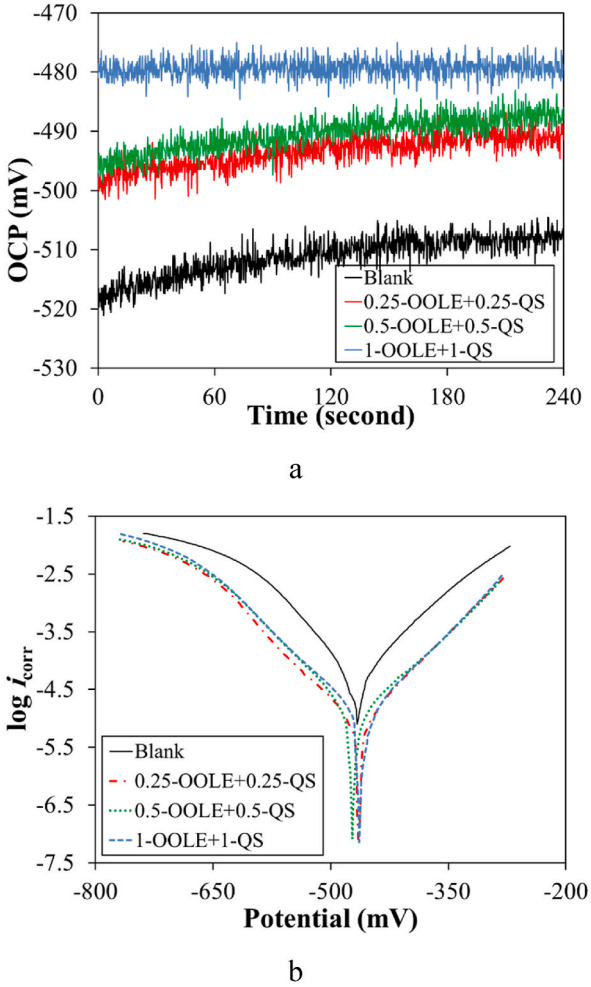

Fig. 3. (a) Plots of OCP versus the immersion time, and (b) log i_{corr} versus potential at 298 K.

presence of bio-inhibitors in the corrosive media. Moreover, Table 2 reports data extracted from the obtained PDP results. This table included corrosion current density (i_{corr}), corrosion potential (E_{corr}), slopes of anodic and cathodic Tafel branches (β_a and β_c), and inhibition efficiency (θ). The E_{corr} range value for all samples was −477.7 to −487.4. The less negative potential was related to the 0.5-OOLE +0.5-QS sample. The event showed a higher tendency to corrosion resistance. Based on the results obtained, it appeared that the bio-inhibitor used in this study acted as a mixed inhibitor, as evidenced by the E_{corr} values being lower than −85 mV for all samples. This finding was consistent with other studies [2,30]. Moreover, changes in values of β_a and β_c were the same. In this manner, both anodic and cathodic reactions were affected by the utilized bio-inhibitor. The bio-inhibitor served as a protective layer that hindered the flow of electrons between the metallic surface and hydrogen ions present in the solution, thus effectively preventing corrosion and ensuring the longevity of the metal. The anodic reaction was $Fe{=}Fe^{2+}+2e^{-}$. The cathodic reaction was also the hydrogen evolution. The range of θ values was about 0.78–0.83, indicating the most effective concentration of inhibitor was 1 gL^{-1}. In other words, the inhibition efficiency percent was about 78–83 %. Based on the adsorption mechanism type (section 3.4), the efficiency did not significantly increase despite the higher amount of inhibitor due to the presence of an adsorption site for each surface atom of the inhibitor molecule, resulting in a nearly unchanged efficiency level. A similar incident has been mentioned in other papers [28,30].

Table 2
Extracted data from the obtained PDP results.

Sample name	i_{corr} (Acm^{-1})	β_a (mV/decade)	β_c (mV/decade)	E_{corr} (mV)	θ
Blank	0.0681 ± 0.0002	71.3 ± 3.0	−107.6 ± 3.0	−482.2 ± 3.0	–
0.25-OOLE+0.25-QS	0.0151 ± 0.0002	76.0 ± 3.0	−111.9 ± 3.0	−487.4 ± 3.0	0.78 ± 0.01
0.5-OOLE+0.5-QS	0.0112 ± 0.0002	69.1 ± 3.0	−110.6 ± 3.0	−477.7 ± 3.0	0.83 ± 0.01
1-OOLE+1-QS	0.0135 ± 0.0002	72.0 ± 3.0	−107.8 ± 3.0	−482.2 ± 3.0	0.80 ± 0.01

3.3. EIS results

Fig. 4 represents the Bode, phase angle, and Nyquist plots of various samples. The addition of bio-inhibitor to the corrosive media led to a significant increase in the impedance modulus (Z) of the steel substrate, as demonstrated in Fig. 4(a). Similar to PDP results, the highest value of Z was attributed to the sample with the optimum inhibitor concentration with a value of 1 g L^{-1}. Fig. 4(b) shows that the lowest phase angle with a value of −75° was related to the 0.5-OOLE +0.5-QS sample, exhibiting a higher corrosion resistance. The lowest phase angle occurred in the frequency range of 10^2–10^3 Hz for all samples; however, in the presence of the bio-inhibitor, the lowest peak shifted to the lower frequencies. Moreover, Fig. 4(c) displays the Nyquist plots of various samples. All diagrams included one semi-ring showing a similar mechanism of corrosion reactions.

To ensure accurate and precise measurements, the EIS data was analyzed using ZView software. The measured data from Bode and phase angle plots is presented in Table 3. The suggested electrical circuit for all samples is illustrated in Fig. 4(a) and consisted of three elements: resistance of 1 M HCl solution (R_s), constant phase element of the double-layer (CPE_{dl}), and polarization resistance (R_p). Due to the roughness of the steel surface, it could not be considered as a flat surface to create a capacitor (C). Instead, CPE was used in the electrical circuit, and the parameter 'n' was introduced to demonstrate the surface roughness. Its value ranged from 0 to 1, where a higher value indicated an ideal surface with the lowest roughness.

The range of R_s values for all samples was 5.6–8.6 Ωcm^2. The highest resistance and the lowest value of CPE_{dl} were attributed to the 0.5-OOLE +0.5-QS sample. The low value of CPE_{dl} indicated a higher thickness of double-layer formed on the metal surface or a lower surface exposed to the corrosive solution. This was based on the capacitor formula [30]. In this situation, the corrosion resistance of the steel substrate increased. Values of n were between 0.85 and 0.89. The 0.5-OOLE +0.5-QS sample exhibited the highest n value, displaying lower corrosion attacks that resulted in lower surface roughness. Values of θ were about 0.83–0.86, indicating the inhibition efficiency percent was about 83–86 %. Based on the findings of previous studies [1,2], variations in inhibitor concentration have been demonstrated to lead to notable changes in the inhibition efficiency. Conversely, results from the EIS analysis suggested that alterations in the mixed inhibitor concentration had an insignificant impact on the inhibition efficiency when the ratio of inhibitors was 1:1. It might be more crucial to adjust the ratio of inhibitors rather than their individual concentrations within the inhibitor mixture, a topic that would be explored in forthcoming research articles.

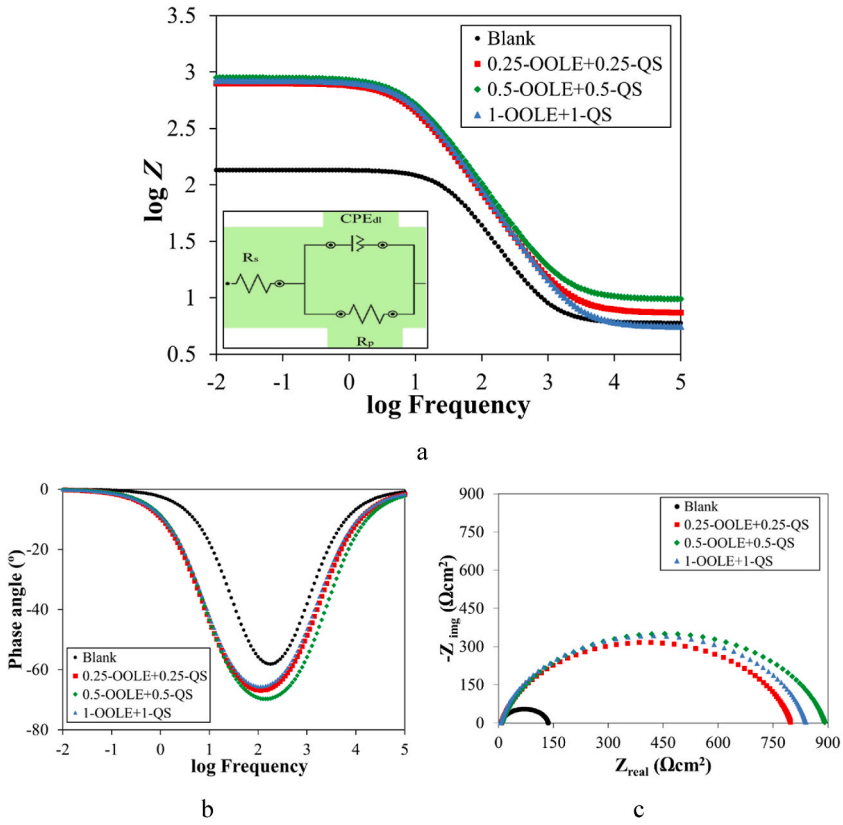

Fig. 4. (a) Bode (b) Phase angle, and (c) Nyquist plots of various samples in 1 M HCl solution at 298 K.

Table 3
Measured EIS data from Bode and phase angle plots.

Sample name	R_s (Ω cm^2)	CPE_{dl} (F cm^{-2})	n	R_p (Ω cm^2)	θ
Blank	6.0 ± 0.3	61.3 ± 4.0	0.85 ± 0.02	129.4 ± 100.0	–
0.25-OOLE+0.25-QS	7.3 ± 0.3	40.6 ± 4.0	0.86 ± 0.02	791.5 ± 100.0	0.83 ± 0.01
0.5-OOLE +0.5-QS	8.6 ± 0.3	39.1 ± 4.0	0.89 ± 0.02	892.5 ± 100.0	0.86 ± 0.01
1-OOLE +1-QS	5.6 ± 0.3	39.9 ± 4.0	0.87 ± 0.02	834.5 ± 100.0	0.84 ± 0.01

3.4. Adsorption mechanism

Based on various parameters like the concentration and type of inhibitor molecules, and the type and temperature of the corrosive environment, the adsorption type could follow different adsorption mechanisms such as Langmuir, Temkin, Flory–Huggins, Freundlich, and Frumkin [1,2]. The Langmuir mechanism was identified when the slope plot of the inhibitor concentration (C) versus the C/θ was linear, as presented in Fig. 5. This linear slope was consistent across all inhibitor concentrations. Moreover, based on values of R^2 (the correlation coefficient [31]), this event showed that the adsorption mechanism was the Langmuir type. In this type, it was supposed that each site on the metal surface could adsorb one constituent of the inhibitor. In this situation, monolayer adsorption of molecule mixture happened. Additionally, no side interaction would be done between the inhibitor and the metal surface [2].

Calculations using the PDP and EIS data were performed with equations (1) and (2) to determine K_{ad} and ΔG°_{ads}, as detailed in Table 4. The negative value of ΔG°_{ads} indicated an exothermic reaction and the spontaneous adsorption of molecules on the metal surface. A similar trend was also reported in other research [28,30]. The analysis suggested that a physical interaction between the mixed inhibitor molecules and the metal surface, primarily driven by van der Waals forces. It was reported that ΔG°_{ads} when the value was less than −20 kJ mol^{-1} physisorption was likely to occur [30].

3.5. FE-SEM

The comparison of the FE-SEM images of the corroded surface in 1 M HCl solution after immersing at 24 h for the blank and 0.5-OOLE+0.5-QS samples (optimum concentration of the utilized inhibitor based on the electrochemical tests) is presented in Fig. 6. The blank sample displayed several holes on its corroded surface and between the corrosion products. These corrosion products were accumulated in an acicular shape, which is similar to the findings of other studies [29]. However, when the bio-inhibitor was added to the corrosive solution, the morphology of the corroded surface changed. The number of holes decreased, indicating a lower corrosion attack than the blank sample. Moreover, Figs. S1 and S2 show EDS mapping results from the corroded surface of both samples. For the sample 0.5-OOLE +0.5-QS, nitrogen and carbon elements were completely uniformly dispersed on the surface, which could indicate the absorption of the inhibitor on the surface.

3.6. MD

Monte Carlo was used to explore the simultaneous presence effect of QS-inhibitor and OOLE-inhibitor for adsorption on the steel surface by calculating the adsorption energy. Fig. 7 shows the 2D structure of the main component in both bio-inhibitor molecules, along with the 3D mode before and after optimization. Notably, it was found that the main species in the OOL and QS extract were chitin with a formula of $(C_8H_{13}O_5N)_n$ [2,32] and starch with a formula of $(C_6H_{10}O_5)_n$ [1,33], respectively. Thus, the main molecules with the highest concentration from each inhibitor were chosen for MD simulations.

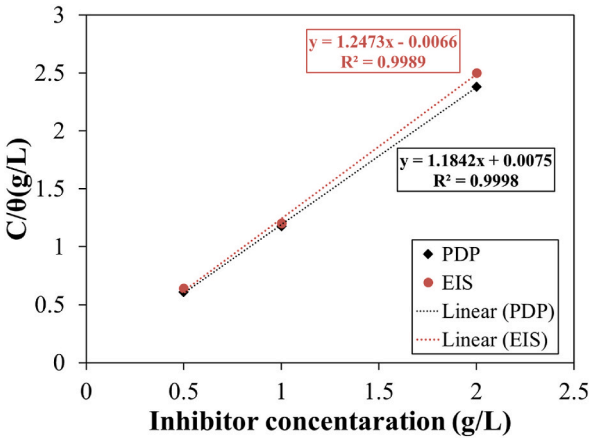

Fig. 5. Plots of inhibitor concentration versus the C/θ to show the Langmuir adsorption mechanism.

Table 4
Calculated data from the.

Calculations based on the PDP data		
Slope of plot (g L^{-1})	K_{ad} (L g^{-1})	ΔG°_{ads} (kJ mol^{-1})
1.18	0.85	−16.7
Calculations based on EIS data		
1.25	0.80	−16.6

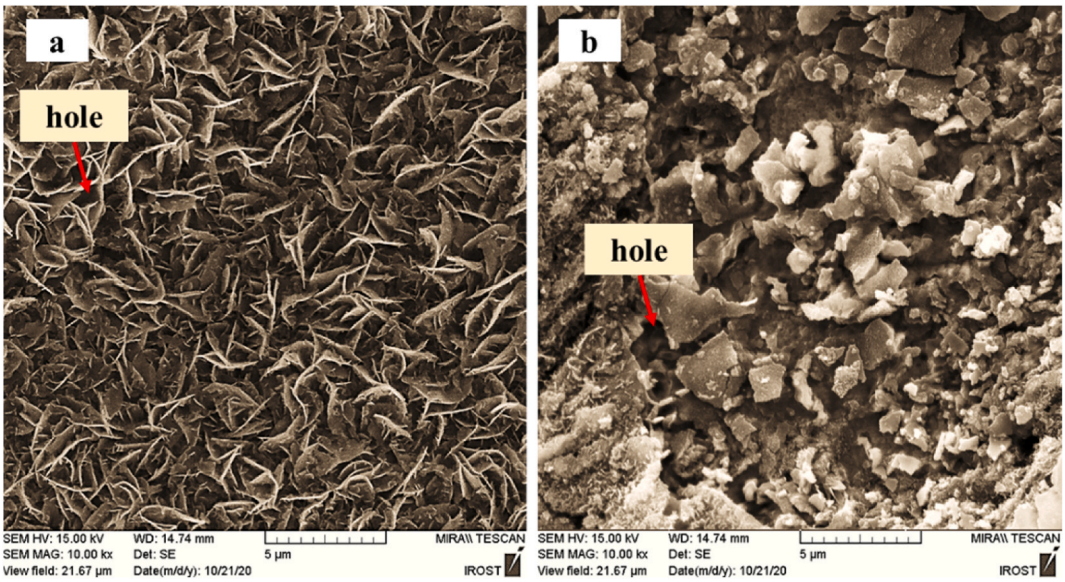

Fig. 6. FE-SEM images of corroded surface in 1 M HCl solution after immersing at 24 h for (a) the blank sample and (b) the sample 0.5-OOLE +0.5-QS.

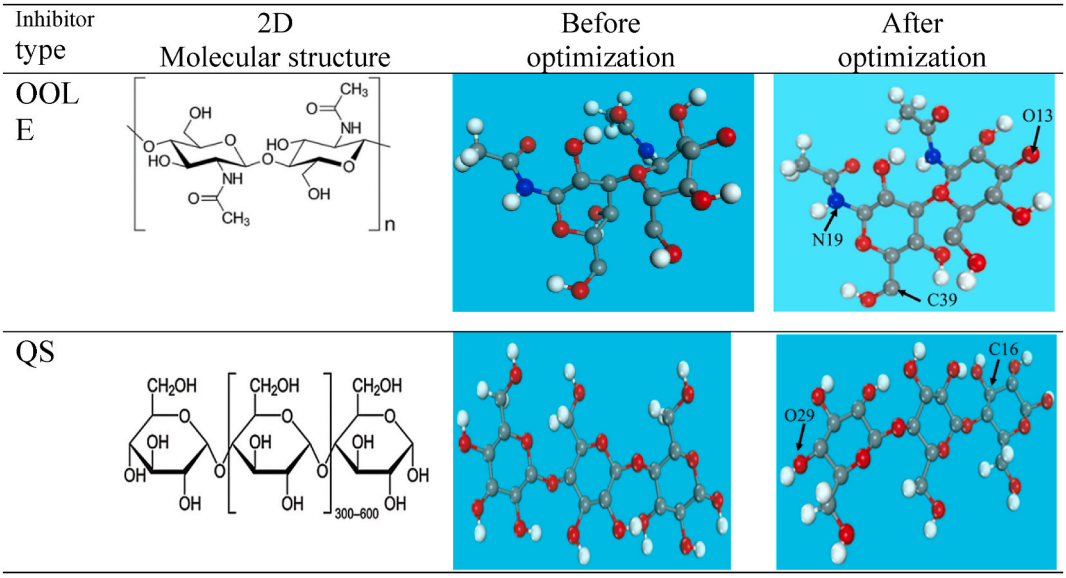

Fig. 7. The structure of inhibitor molecules before and after optimization.

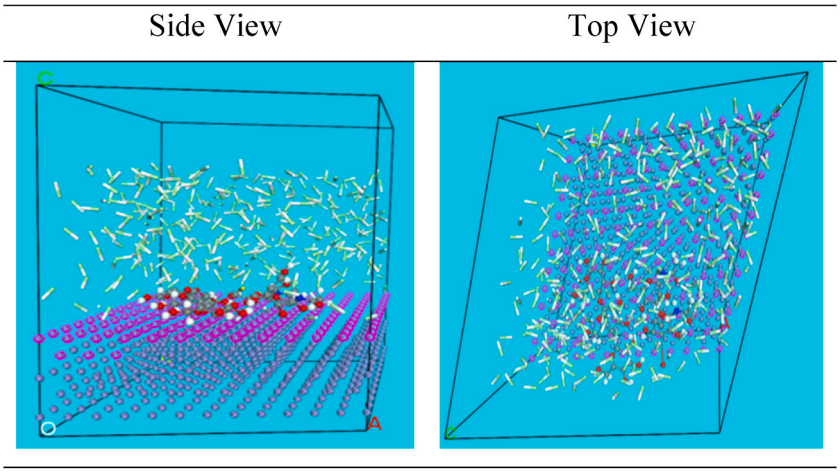

Fig. 8. MD simulation showing QS-inhibitor and OOLE-inhibitor molecules co-adsorption on Fe (110) in side and top view.

Table 5
Different values of energy in kcal mol^{-1} were obtained from MD simulation using Monte Carlo calculations for the adsorption of inhibitor molecules on Fe (110).

Inhibitor molecule	Total energy	Binding energy	Rigid adsorption energy	Deformation energy	OOLE: dEad/dNi	QS: dEad/dNi
Mixed inhibitor	−187.31	−366.45	−378.83	12.38	−160.61	−216.16
QS-inhibitor	−101.38	−220.98	−252.97	31.99	–	−220.98
OOLE-inhibitor	−173.01	−161.01	−163.69	2.68	−161.01	–

Fig. 8 presents MD simulations, indicating the co-adsorption of QS-inhibitor and OOLE-inhibitor molecules on Fe (110) in both side and top views. The adsorption energies of these inhibitors are calculated and reported in Table 5. As displayed in Fig. 8, both bio-inhibitors were in one parallel direction when adsorbed at the Fe (110) surface. The results showed that the adsorption of both bio-inhibitors caused an inhibition effect for the steel corrosion as the negative adsorption energies represented that the adsorption of both bio-inhibitors on the steel surface could occur spontaneously [34]. The most negative (lowest) adsorption energy was related to the mixed inhibitor. Moreover, the more negative adsorption energy of the QS-inhibitor compared to the OOLE-inhibitor, led to stronger interaction of the QS-inhibitor on the Fe (110) surface, and resulted in a higher inhibition efficiency than OOLE-inhibitor molecules. A similar consequence was also found in other research [35]. Overall, the results suggested that the QS-inhibitor had a greater effect than the OOLE-inhibitor, which aligned with the experimental results in previous studies [1,2]. Additionally, the deformation energy was highest for the QS-inhibitor; however, the binding energy was highest in the presence of the mixture of the utilized inhibitor.

3.7. Quantum chemical calculation

At first, inhibitor molecules were optimized with DMOl3, and then with Task: Energy. Then, the results related to the highest occupied molecular orbital (HOMO), the lowest unoccupied molecular orbital (LUMO), the electrostatic potential (ESP), and Fukui indices were obtained. According to molecular orbitals theories, the transfer of electrons is related to HOMO and LUMO of a molecule. The HOMO energy represents the ability of a molecule to donate electrons to an acceptor exhibiting vacant orbitals, while the LUMO energy value indicates the ability of a molecule to accept electrons. In this regard, the higher HOMO energy value results in a stronger electron-donating ability of a molecule, and higher corrosion resistance [36]. On the other hand, the lower LUMO energy shows that the molecule accepts electrons easily. Fig. 9 demonstrates the HOMO and LUMO structures for both bio-inhibitor molecules, along with the regions that included electron donation and acceptance. The brown color presented a high electron density, while the yellow one displayed a lower electron density. For the QS-inhibitor molecule, the HOMO and the LUMO were located on the cyclic carbon group in the middle of and on the side of the structure, respectively. However, for OOLE-inhibitor molecule, both LUMO and HOMO were presented on the hydroxyl group. A similar observation was also found in other research [36].

Table 6 contains the calculated properties of utilized molecules, including HOMO and LUMO energies, ΔE, I, A, χ, η, as well as ΔN. The findings suggested that a suitable corrosion inhibitor molecule exhibited a low energy level of LUMO and a high energy level of HOMO [37]. In this case, the highest HOMO level was related to QS-inhibitor which supported the effect of this molecule in adsorbing at the steel surface and as a result, enhanced the inhibition efficiency. On the other hand, the lower value of the LUMO was attributed to the OOLE-inhibitor.

Moreover, it was found that a lower energy gap indicated a higher reactivity or efficiency of the inhibitor [36,38]. In total, the reactivity and efficiency of the QS-inhibitor molecule with the steel surface were found to be higher compared to the OOLE-inhibitor,

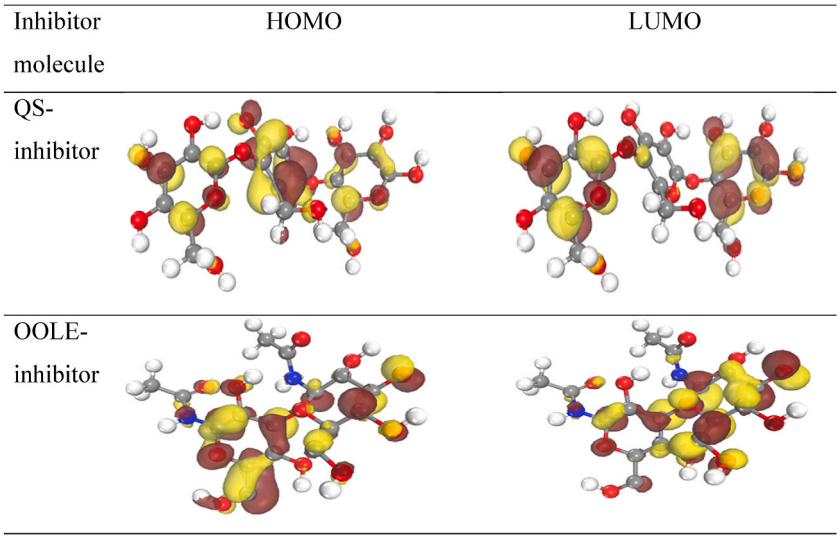

Fig. 9. HOMO and LUMO structure for utilized bio-inhibitors.

Table 6
Quantum chemical parameters for inhibitory molecules (in terms of ev).

Inhibitor molecule	E_{HOMO}	E_{LUMO}	ΔE_{gap}	I	A	χ	η	Δn
QS-inhibitor	−2.84	−2.64	0.20	2.84	2.64	2.74	0.10	20.87
OOLE-inhibitor	−5.04	−4.77	0.27	5.07	4.77	4.90	0.13	7.88

based on the lower value of ΔE. Inhibitors often exhibited a low value of A, presenting a capability for electron donations to the metal surface [37]. In this case, the QS-inhibitor molecule could adsorb faster than the OOLE-inhibitor. The activity and durability of a molecule could be studied through parameters such as χ and η. Soft molecules were more suitable inhibitors as they could more easily transfer electrons to the surface when adsorbed [37]. Thus, the OOLE-inhibitor showed higher durability compared to the QS-inhibitor. Additionally, it was found that when the value of ΔN was positive, the tendency of electron transfer between the metal and the inhibitor was higher. In this situation, both bio-inhibitors exhibited a high likelihood of the electron transfer. However, the QS-inhibitor molecule had a higher value of ΔN than the OOLE-inhibitor, indicating a high number of electrons that were transferred to interact

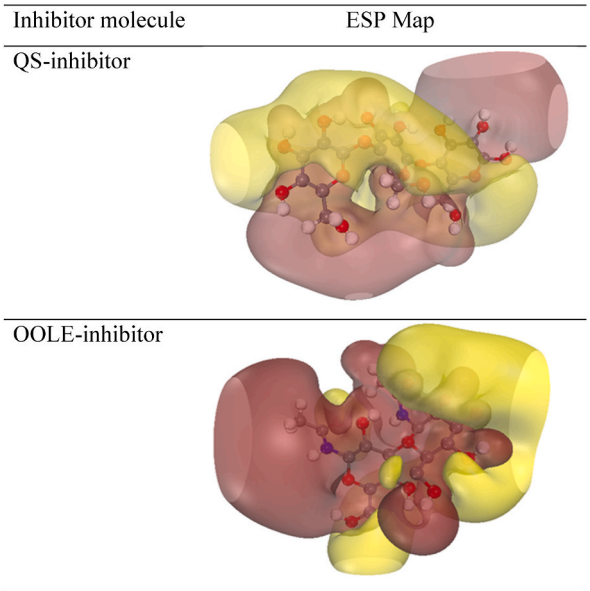

Fig. 10. Electrostatic potential structure (ESP) of both bio-inhibitor molecules.

with the metal surface. Overall, these findings suggested that the QS-inhibitor molecule has a higher reactivity and efficiency, while the OOLE-inhibitor exhibits better durability.

ESP of QS-inhibitor and OOLE-inhibitor molecules is displayed in Fig. 10. The brown part represented the positive electrostatic potential, whereas the yellow-colored area indicated the negative potential. It was found that the nucleophilic potential (in brown) played a crucial role in the adsorption process on the metal surface. In other words, the ESP determined the direction of molecule adsorption on the metal surface. For the QS-inhibitor, the direction was toward oxygen atoms located at the end of the structure. On the other hand, for the OOLE-inhibitor, this direction was towards the cyclic carbonic group and nitrogen atoms.

To analyze the interaction between inhibitory molecules of electrophilic or nucleophilic type, quantum calculations were used which involve calculating electrons at a constant external potential [39]. By using the Fukui indices, the active centers of the molecule in the optimized structure for receiving and donating electrons were determined, as shown in Fig. 11. The results obtained from the values of the Fukui indices for the attack of electrophilicity (f^-) and nucleophilicity (f^+), displayed the atoms that were most exposed to attack [38], and the findings are reported in Table S1. In other words, it was determined that the f^+ signified the location where the molecule was most susceptible to an electrophilic attack, while the (f^-) indicated the site most prone to a nucleophilic attack [40]. The electron attack and nucleophilicity mostly belonged to the atoms C16 and O29 of the QS-inhibitor and N19, O13, and C39 of the OOLE inhibitor. Notably, C39 was associated with the carbon atom bonded to a phenolic group. O13 was part of a carbon cyclic group with high electron density. C16 was within the cyclic group, while O29 was outside a carbon cyclic group but attached to it. Wherever the amount of electrophilicity increased, it meant electron capture and the inhibition occurred from that side. Overall, the findings aligned with the experimental calculations.

4. Conclusions

In this paper, as a new study, the mixture effect of two bio-inhibitors on the electrochemical property of the carbon steel in 1 M HCl solution was investigated. The total inhibitor concentration was between 0.5 and 2 g L^{-1}, as a variable factor. Moreover, MD and quantum mechanics (QM) simulations were performed for the adsorption of QS-inhibitor and OOLE-inhibitor molecules on the Fe (110) surface. The obtained results were summarized, as follows.

- The corrosion resistance of carbon steel increased by 83–86 % in the presence of the bio-inhibitor mixture, based on the EIS measurements. The optimum concentration was 1 g L^{-1} (0.5-OOLE +0.5-QS). The adsorption mechanism was obeyed from the Langmuir model and acted as a mixed inhibitor. Based on the value of ΔG°_{ads} (−16.7 kJ mol^{-1}), the bonding of steel surface and inhibitor molecules was physical and van der Waals. FE-SEM images also confirmed fewer corrosion attacks on the steel surface when bio-inhibitor was added to the corrosive solution.
- MD results indicated that in the presence of both bio-inhibitors, the steel inhibition would have occurred. However, the QS-inhibitor was first adsorbed on the metal surface and had a greater effect. Moreover, the lowest calculated adsorption energy was related to the mixed inhibitor. Both bio-inhibitors were in one parallel direction when adsorbed at the Fe (110) surface.

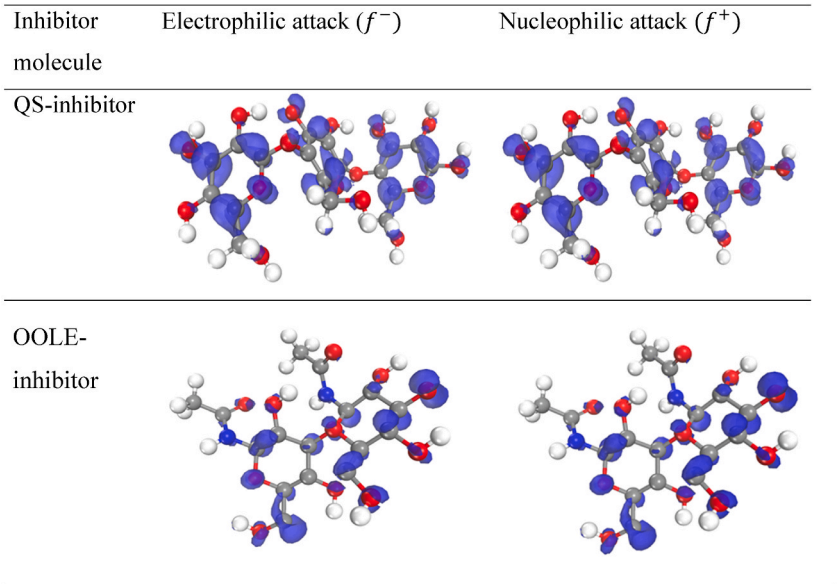

Fig. 11. Electrophilic attack of f^- and nucleophilic attack f^+ for both inhibitory molecules.

- Quantum calculations based on density functional theory (DFT) showed that carbon in the cyclic structure and oxygen molecules compared to nitrogen molecules were active sites for adsorption of the bio-inhibitor mixture and resulted in a reduction in corrosion attacks, which was also confirmed by the experimental results.

CRediT authorship contribution statement

Amirhossein Hafazeh: Software, Investigation. **Haneih Mobtaker:** Methodology, Investigation. **Mahboobeh Azadi:** Writing – review & editing, Writing – original draft, Supervision. **Maryam Rassouli:** Methodology.

Data availability statement

Data will be made available on request.

Declaration of competing interest

The authors declare that they have no known competing financial interests or personal relationships that could have appeared to influence the work reported in this paper.

Appendix A. Supplementary data

Supplementary data to this article can be found online at https://doi.org/10.1016/j.heliyon.2024.e39066.

References

[1] H. Mobtaker, M. Azadi, N. Hassani, M. Neek-Amal, M. Rassouli, M.A. Bidi, The inhibition performance of quinoa seed on corrosion behavior of carbon steel in the HCl solution; theoretical and experimental evaluations, J. Mol. Liq. 335 (2021) 16183.
[2] H. Mobtaker, M. Azadi, M. Rassouli, The corrosion inhibition of carbon steel in 1 M HCl solution by Oestrus ovis larvae extract as a new bio–inhibitor, Heliyon 8 (12) (2022) 12297.
[3] M. Mehdipour, B. Ramezanzadeh, S.Y. Arman, Application of electrochemical noise to investigate corrosion inhibition properties of some azole compounds on aluminum in 0.25 M HCl, Progress in Color, Colorants and Coatings 8 (2014) 69–86.
[4] H. Lgaz, R. Salghi, K.S. Bhat, A. Chaouiki, S. Jodeh, Correlated experimental and theoretical study on inhibition behavior of novel quinoline derivatives for the corrosion of mild steel in hydrochloric acid solution, J. Mol. Liq. 244 (2017) 154–168.
[5] H. Lgaz, K.S. Bhat, R. Salghi, S. Jodeh, M. Algarra, B. Hammouti, I.H. Ali, A. Essamri, Insights into corrosion inhibition behavior of three chalcone derivatives for mild steel in hydrochloric acid solution, J. Mol. Liq. 238 (2017) 71–83.
[6] H. Lgaz, R. Salghi, S. Jodeh, B. Hammouti, Effect of clozapine on inhibition of mild steel corrosion in 1.0 M HCl medium, J. Mol. Liq. 225 (2017) 271–280.
[7] P. Dohare, M. Quraishi, C. Verma, H. Lgaz, R. Salghi, E. Ebenso, Ultrasound induced green synthesis of pyrazolo-pyridines as novel corrosion inhibitors useful for industrial pickling process: experimental and theoretical approach, Results Phys. 13 (2019) 102344.
[8] M. Kundu, S.K. Prasad, V. Kumar, A review article on green inhibitors of reinforcement concrete corrosion, International Journal of Emerging Research in Management and Technology 5 (1) (2016) 42–47.
[9] G. khan, K.M.S. Newaz, W.J. Basirun, H.B.M. Ali, F.L. Faraj, G.M. Khan, Application of natural product extracts as green corrosion inhibitors for metals and alloys in acid pickling processes- A review, Int. J. Electrochem. Sci. 10 (2015) 6120–6134.
[10] Y. Qiang, S. Zhang, B. Tan, S. Chen, Evaluation of Ginkgo leaf extract as an eco-friendly corrosion inhibitor of X70 steel in HCl solution, Corrosion Sci. 133 (2018) 6–16.
[11] A.R. Torres, M.G.V. Cisneros, J.G.G. Rodrigueza, Medicago sativa as a green corrosion inhibitor for 1018 carbon steel in 0.5 M H2SO4 solution, Green Chem. Lett. Rev. 9 (3) (2016) 143–155.
[12] H. Bourazmi, M. Tabyaoui, L.E. Hattabi, Y.E. Aoufir, M. Taleb, Methanolic extract of salvia officinalis plant as a green inhibitor for the corrosion of carbon steel in 1 M HCl, Journal of Materials and Environmental Sciences 9 (3) (2018) 928–938.
[13] S. Varvara, R. Bostan, O. Bobis, L. Gaina, F. Popad, V. Menae, R.M. Soutoe, Propolis as a green corrosion inhibitor for bronze in weakly acidic solution, Appl. Surf. Sci. 426 (2017) 1100–1112.
[14] R.S. A Kumari, V. Chandrasekaran, Sargassum wightii extract as a green inhibitor for corrosion of brass in 0.1 N phosphoric acid solution, Orient. J. Chem. 31 (2) (2015) 939–949.
[15] O.K. Abiola, A.O. James, The effects of Aloe vera extract on corrosion and kinetics of corrosion process of zinc in HCl solution, Corrosion Sci. 52 (2010) 661–664.
[16] K.C. Emregul, M. Hayval, Studies on the effect of vanillin and protocatechualdehyde on the corrosion of steel in hydrochloric acid, Mater. Chem. Phys. 83 (2–3) (2004) 209–216.
[17] Z.G. Luo, Y. Zhang, H. Wang, S. Wan, L.F. Song, B.K. Liao, X.P. Guo, Modified nano-lignin as a novel biomass-derived corrosion inhibitor for enhanced corrosion resistance of carbon steel, Corrosion Sci. 227 (2024) 111705.
[18] N.S. Abdelrahman, E. Galiwango, A.H. Al-Marzouqi, E. Mahmoud, Sodium lignosulfonate: a renewable corrosion inhibitor extracted from lignocellulosic waste, Biomass Conversion and Biorefinery 14 (2024) 7531–7541.
[19] M.A. Bidi, M. Azadi, M. Rassouli, A new green inhibitor for lowering the corrosion rate of carbon steel in 1 M HCl solution: hyalomma tick extract, Mater. Today Commun. 24 (2020) 100996.
[20] J. Bhawsar, P.K. Jain, P. Jain, Experimental and computational studies of Nicotiana tabacum leaves extract as green corrosion inhibitor for mild steel in acidic medium, Alex. Eng. J. 54 (2015) 769–775.
[21] Y. Qiang, S. Zhang, B. Tan, S. Chen, Evaluation of Ginkgo leaf extract as an ecofriendly corrosion inhibitor of X70 steel in HCl solution, Corrosion Sci. 133 (2018) 6–16.
[22] H. Lgaz, R. Salghi, Ismat H. Ali, Corrosion inhibition behavior of 9-Hydroxyrisperidone as a green corrosion inhibitor for mild steel in hydrochloric acid: electrochemical, DFT and MD Simulations Studies, Int. J. Electrochem. Sci. 13 (2018) 250–264.
[23] K.O. Sulaiman, A.T. Onawole, O. Faye, D.T. Shuaib, Understanding the corrosion inhibition of mild steel by selected green compounds using chemical quantum based assessments and molecular dynamics simulations, J. Mol. Liq. 279 (2019) 342–350.

[24] M. Alahiane, R. Oukhrib, Y.A. Albrimi, H.A. Oualid, R. Idouhli, A. Nahle, A. Berisha, N.Z. Azzallou, M. Hamdani, Corrosion inhibition of SS 316L by organic compounds: experimental, molecular dynamics, and conceptualization of molecules–surface bonding in H2SO4 solution, Appl. Surf. Sci. 612 (2023) 155755.
[25] P. Singh, M. Kumar, M. Ahmad Quraishi, J. Haque, G. Singh, Bispyranopyrazoles as green corrosion inhibitors for mild steel in hydrochloric acid: experimental and theoretical approach, ACS Omega 3 (2018) 11151–11162.
[26] M. Rassouli, M. Azadi, Parasites as metal corrosion inhibitors, new achievements, Current Green Chemistry 10 (2) (2023) 105–108.
[27] M.A. Bidi, M. Azadi, M. Rassouli, Comparing the inhibition efficiency of two bio-inhibitors to control the corrosion rate of carbon steel in acidic solutions, Analytical and Bioanalytical Electrochemistry 13 (1) (2021) 52–66.
[28] M.A. Bidi, M. Azadi, M. Rassouli, An enhancement on corrosion resistance of low carbon steel by a novel bio-inhibitor (leech extract) in the H2SO4 solution, Surface. Interfac. 24 (2021) 101159.
[29] M. Akbari Shahmirzadi, M. Azadi, A new study on the corrosion inhibition mechanism of green walnut husk extract as an agricultural waste for steel protection in HCl solution Heliyon10 (9) (2024) 29962.
[30] B. Jafari, M. Yousefpour, M. Azadi, The inhibition effect of white dextrin on Al1050 alloy corrosion behavior in the NaOH media: thermodynamic and kinetic study, J. Indian Chem. Soc. 100 (10) (2023) 101089.
[31] S. Safarloo, F. Loghman, M. Azadi, M. Azadi, Optimal design experiment of ageing time and temperature in Inconel-713C superalloy based on hardness objective, Transactions of the Ind ian Institute of Metals 71 (2018) 1563–1572.
[32] M. Meneguz, A. Schiavone, F. Gai, A. Dama, C. Lussiana, M. Renna, L. Gasco, Effect of rearing substrate on growth performance, waste reduction efficiency and chemical composition of black soldier fly (Hermetia illucens) larvae, J. Sci. Food Agric. 98 (2018) 5776–5784.
[33] J.A. Gonzalez, A. Roldan, M. Gallardo, T. Escudero, F.E. Praddo, Quantitative determinations of chemical compounds with nutritional value from Inca crops: Chenopodium quinoa ('quinoa'), Plant Foods Hum. Nutr. 39 (1989) 331–337.
[34] M. El housse, A. Hadfi, I. Karmal, B. EL Ibrahimi, S. Ben-aazza, M. Errami, M. Belattar, S. Mohareb, A. Driouiche, Experimental investigation and molecular dynamic simulation of Tannic acid as an eco-friendly inhibitor for calcium carbonate scale, J. Mol. Liq. 340 (2021) 117225.
[35] M. Abdallah, K.A. Soliman, B.A. Al Jahdaly, J.H. Al-Fahemi, H. Hawsawi, H.M. Altass, M.S. Motaweabd, S.S. Al-Juaid, Natural parsley oil as a green and safe inhibitor for corrosion of X80 carbon steel in 0.5 M H(2)SO(4) solution: a chemical, electrochemical, DFT and MC simulation approach, RSC Adv. 12 (5) (2022) 2959–2971.
[36] Y. Zhu, S. Qu, Y. Shen, X. Liu, N. Lai, Z. Dai, J. Liu, Investigation on the synergistic effects and mechanism of oleic imidazoline and mercaptoethanol corrosion inhibitors by experiment and molecular dynamic simulation, J. Mol. Struct. 1274 (2023) 134512.
[37] K. Shalabi, H.M. Abd El-Lateef, M.M. Hammouda, A.A. Abdelhamid, Green synthesizing and corrosion inhibition characteristics of azo compounds on carbon steel under sweet conditions: experimental and theoretical approaches, ACS Omega 9 (17) (2024) 18932–18945.
[38] S.K. Saha, M. Murmu, P. Banerjee, Evaluating electronic structure of quinazolinone and pyrimidinone molecules for its corrosion inhibition effectiveness on target specific mild steel in the acidic medium: a combined DFT and MD simulation study, J. Mol. Liq. 224 (2016) 629–638.
[39] A.A. Khadom, M.M. Kadhim, R.A. Anaee, H.B. Mahood, M.S. Mahdi, A.W. Salman, Theoritical evaluation of Citrus Aurantium leaf extract as green inhibitor for chemical and biological corrosion of mild steel in acidic solution: statistical, molecular dynamics, docking, and quantum mechanics study, J. Mol. Liq. 343 (2021) 116978.
[40] A. Rizi, A. Sedik, A. Acidi, K.O. Rachedi, H. Ferkous, M. Berredjem, A. Delimi, A. Abdennouri, M. Alam, B. Ernst, Y. Benguerba, Sustainable and green corrosion inhibition of mild steel: insights from electrochemical and computational approaches, ACS Omega 8 (49) (2023) 47224–47238.